AMAS Course on Nondestructive Testing of Materials
NTM'02 – (pp.137–157) – Warsaw, May 20-22, 2002.

Application of metal magnetic memory method for examination of welded joints

J. KORZENIOWSKI, Z. ŁAPIŃSKI and P. ONISZK

Military Institute of Armament Technology
Zielonka, Poland
witu@witu.mil.pl

A new metal magnetic memory non-destructive testing method based on detection and measurement of residual magnetic fields of scattering in ferromagnetic material is presented in the paper. The usefulness of the method was presented by measurement results obtained from two groups of samples, the first one concerns especially prepared testing samples and the second deals with real parts being long-term in service.

1. Introduction

Traditional diagnostic methods (magnetic, X-ray inspection, penetration) enable the detection of developed defects. Modern methods which allow the detection of potential points of construction where different kinds of defects may appear become more and more important. Such detection ensures safe operation of the whole construction in real conditions by elimination of defects that may lead to catastrophic changes of characteristics in used materials.

Equipment with guarantee or safe operation time expired constitutes a separate problem. As the number of such objects increases in the national and defence industry the evaluation of possibilities and conditions for safe and reliable operation is becoming a very important problem.

2. Method description

One of the methods which gives a solution for the above problems and requirements is the metal magnetic memory one and it belongs to non-destructive testing group. The method is based on disclosing of residual magnetic fields of scattering in ferromagnetic materials which are generated by

the Earth magnetic field in places of stress concentration caused by working load.

Such areas are detected on the surface of tested object as magnetic anomalies generating so called magnetic fields of scattering at places of concentration of stress and deformation.

The residual magnetism disappears in the manufacturing processes of ferromagnetic goods when accompanied technological processes such as melting, forging and heat treating at temperatures higher than Curie point are applied. Following the cooling process the magnetic texture of metal is generated below 768°C degrees in the Earth magnetic field. In such a way a structural shape of metal and its technological "history" are disclosed in the form of magnetic memory, see Fig. 1.

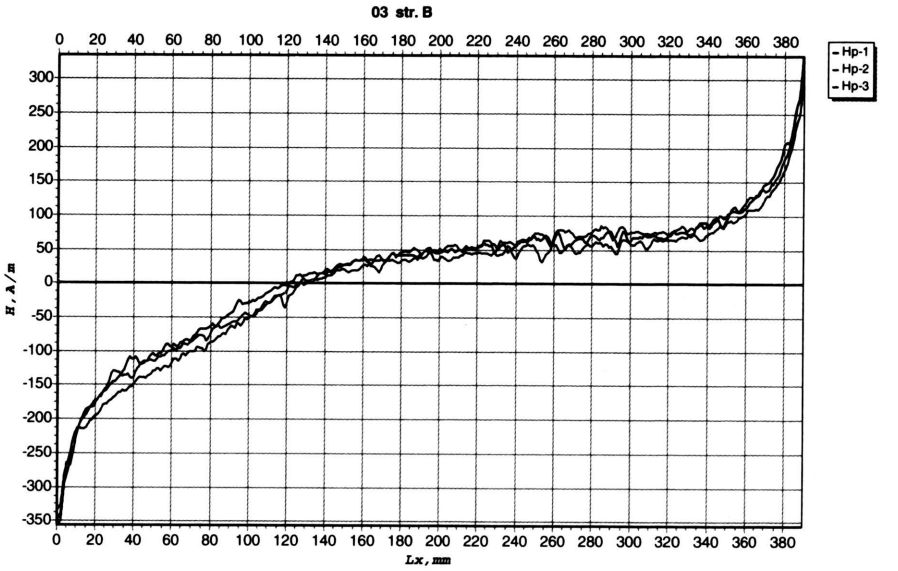

FIGURE 1. Distribution of residual magnetism for the element without clear defects. Lx – distance to the point indicating the start of scanning, H – normal component of magnetic field intensity.

Generally the magnetic metal memory is a magnetisation status caused by stresses which are above the mean level and which appears when different types of strains are acting in the Earth magnetic field.

Mechanical stresses acting in the service time can change significantly the value and distribution of residual magnetism especially in small external magnetic fields (the Earth field), when the magnetisation level of the object is far below the saturation.

Zones of stress concentration are always generated in the complex stress situation and are placed usually in the vicinity of material discontinuities where the resultant deformations are maximal. There is the biggest change of magnetic induction in these zones which generates an additional field of scattering ΔH_r.

The action of working strains and rapid change of magnetic induction not only increase the signal originating from zones with defects but also disclose the stress concentration zones where the processes of corrosion, fatigue and creep in the material are more intensive and what may lead in effect to defects or failures during the further functioning of equipment.

The inspection process using this method is based on the measurement of the component of the scattering field H_r^y which is perpendicular to the surface of the object. It was experimentally verified that the sign change line of H_r^y exists in zones where the defect develops in metal. The line $H_r^y = 0$ was accepted as a diagnostic parameter. It corresponds to the section of tested object with maximum magnetic resistance and reflects the zone of intense material structure discontinuity and in the end maximum internal stress concentration (KN), see Fig. 2.

The stretching tests show that position of the KN line coincides with the zones where the greatest number of elastic deformation traces is disclosed. It was shown that after gaining the load which equals $\sim 0.6\sigma_{pl}$ and further to the plasticity limit σ_{pl} the value of the normal component H_r^y and its gradient in practice remain unchanged. It is connected with the sliding of metal layers in the KN zone. The investigations of samples along the stress concentration line show that these zones are characterised by increased density of dislocation.

The effects of stress and magnetostriction fulfill the following equation:

$$\frac{1}{l}\left(\frac{\partial l}{\partial H}\right)_{\sigma} = \left(\frac{\partial H}{\partial \sigma}\right)_{H}. \tag{2.1}$$

The existing field of scattering can be described with sufficient accuracy by the field of point dipole, provided that material is homogeneously magnetised:

$$H_r^y = m\left\{\frac{r}{[(x+l)^2+r^2]^{3/2}} - \frac{r}{[(x-l)^2+r^2]^{3/2}}\right\}, \tag{2.2}$$

where:

H_r^y – the normal component of the scattering field,

m – the magnetic charge of dipole,

$2l$ – the base of dipole,

r – the distance between sensor and the axis of dipole.

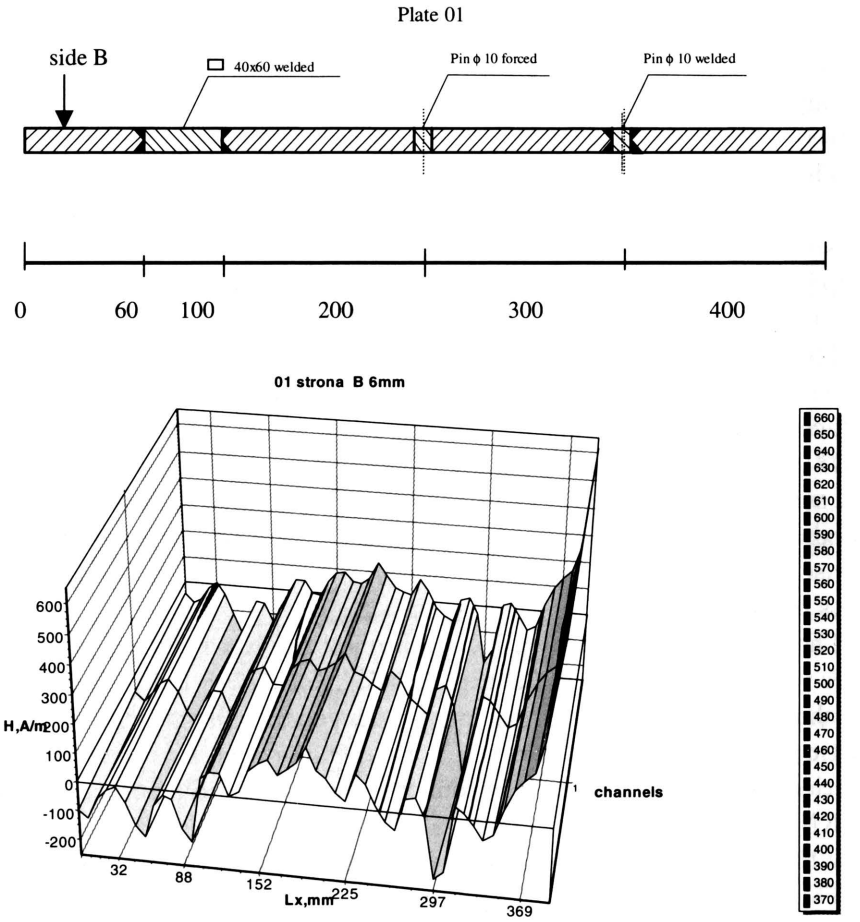

FIGURE 2. Distribution of residual magnetism for the plate 01.

In the case of welded joints the generation of the magnetic domain structure occurs simultaneously with crystallisation at the metal cooling in the Earth magnetic field by the transition of the Curie point. The fixing nods of domains are placed in joint defects when such are generated and they form the magnetic field of scattering above the surface. In this way the possibility for real evaluation of welded joint status by detection of mentioned fields was generated. And the magnetic metal memory reflects exactly all defects and real residual stresses.

Under the influence of working loads metal "remembers" the zone of maximal stresses and deformations. Such very durable change of magnetisation in the zones of maximum working load action and also a resultant magneti-

sation of goods and welded joints after making them was called as "Metal Magnetic Memory".

The investigations performed allow us to state that the value of magnetic field of scattering in each investigated point is described by the tensor of magnetic permittivity that corresponds to the tensor of residual stresses and deformation.

At the present stage of research the above method gives no simple and quantitative evaluation of acting (or residual) stresses.

However, it enables to evaluate:

- degree of contamination of welded joints by defects (number of such places) and to indicate the presence of developing defects,
- distribution of remaining (residual) stresses and stress concentration zones,
- quality and effectiveness of thermal processing.

The defects of technological original can be found in the welded joint such as gaseous pores, slag inclusions and lack of melting, etc. Their presence creates conditions for appearing some additional and local stress concentration zones when they are exposed to complex static and cyclic loads during service life.

Changes of conditions and metal microstructure in the stress concentration zones (weld seam material, heat zone effect, original material) are favourable processes which generate defects in welded joints. There is the correspondent change of metal magnetisation that reflects strain – deformation status of joints.

In the case of welded joints, the intensity of magnetic field of scattering H_r^y is proposed as a parameter describing residual magnetism distribution. Its distribution may characterise an unsatisfactory status of joint with clearly indicated residual stress concentration zones.

The gradient (intensity of changes) of normal component of magnetic field H_r^y at the vicinity of the line $H_r^y = 0$ is used for quantitative evaluation of stress concentration level:

$$K_{in} = \frac{|\Delta H_r^y|}{2l_k}, \tag{2.3}$$

where:

$|\Delta H_r^y|$ – the absolute value of H_r field intensity difference between two measurement points, situated at the same distances l_k on both sides of the $H_r^y = 0$ line,

l_k – the distance between inspection points situated at the same distances from the line $H_r^y = 0$ and normal to it.

The coefficient K_{in} describes the intensity of material magnetisation status change in the KN zone and indirectly the residual stress intensity.

In order to describe stress concentration zones placed across (along the width) the welded joint the following coefficient is used:

$$K^{\delta}_{\max} = \frac{|\Delta H^{\delta}_r|}{\Delta l\sigma}, \tag{2.4}$$

where:

$|H^{\delta}_r|$ – the maximum magnetic field intensity difference between two sensors (measurement channels: H_r – 1 and H_r – 2), if the base distance Δl_σ between them equals the width of welded joint.

By using multi-channel sensors, K_{in} on the plane given by:

$$K_{in} = \sqrt{\left[\frac{|\Delta H^{y}_r|^{ij}}{l^{ij}_k}\right]^2 + \left[\frac{|\Delta H^{y}_r|^{if}}{l^{if}_\sigma}\right]^2} \tag{2.5}$$

where:

f – number of sections between adjacent measurement channels,

$i = 1, 2, 3, \ldots$ – consecutive inspection points for particular measurement channel,

j – measurement channel number,

l^{ij}_k – distance between the i-th and (i – 1) inspection point for the j-th measurement channel,

l^{ij}_σ – distance between adjacent measurement channels for the i-th measurement on the f-th section,

$|\Delta H_r|^{ij}$ – H_r absolute difference value between the i-th and the $(i-1)$-th inspection point for the j-th measurement channel,

$|\Delta H_r|^{if}$ – H_r absolute difference value on the f-th section between adjacent channels for the i-th measurement.

The sections of welded joints where maximally sign-changing distribution of the field intensity H_r was observed for particular channels or the maximum value for the coefficient of $K_{in} = dH_r/dx$. The field intensity change for any measurement channel observed are the most susceptible to develop the defects.

In the case where defects are not detected in the stresses concentration zone or those detected are acceptable then such zones will be qualified to the first order inspection group at the next time.

Some tests and investigations presented below were carried out by using the above method.

3. Application of the method and its evaluation

3.1. Steel plate 01 made from low carbonised steel (Figs. 3 and 4)

The above plate was processed in the following way:

- the element with rectangular cross-section and dimensions of 40 × 60 mm was welded in,

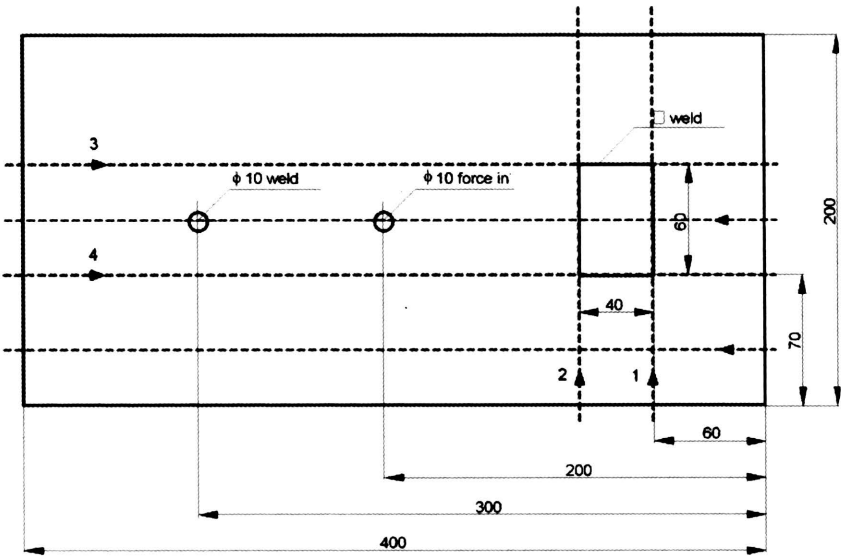

FIGURE 3. Plate 01 with designed defects.

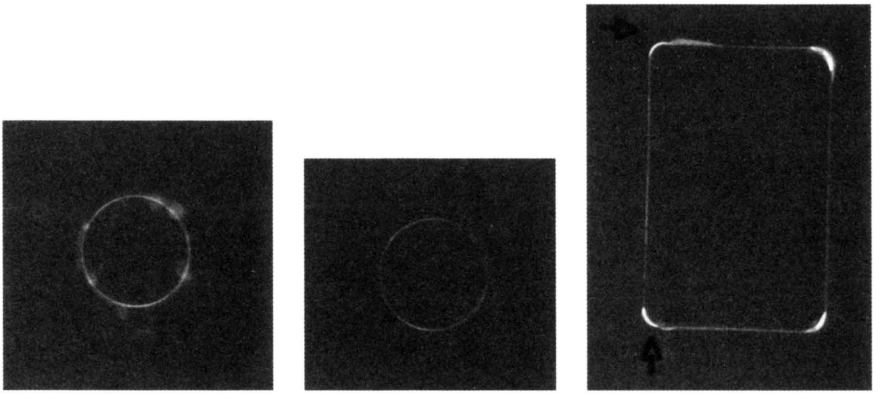

FIGURE 4. X-ray scans of plate 01 with defects.

- the pin of 10 mm diameter was forced in,
- the pin of 10 mm diameter was welded in.

Results of tests are presented in Figs. 5, 6 and 7 and in Table 1.

TABLE 1.

No.	Type of defect	No. of channel	H	$\lvert H_2-H_1\rvert$	$\lvert H_2-H_3\rvert$	$\lvert H_1-H_3\rvert$	$K_{\max}$
1/01	Plate 01, right lower corner, line 1, 70 mm	H_r-1	300.0	100.0	37.0	137.0	16.0
		H_r-2	200.0				6.5
		H_r-3	163.0				2.0
2/01	Plate 01, right upper corner, line 1, 130 mm	H_r-1	120.0	20.0	24.0	44.0	30.0
		H_r-2	100.0				13.7
		H_r-3	76.0				3.8
3/01	Plate 01, left lower corner, line 2, 70 mm	H_r-1	80.0	72.0	48.0	120.0	13.0
		H_r-2	152.0				11.0
		H_r-3	200.0				25.0
4/01	Plate 01, right upper corner, line 2, 130 mm	H_r-1	80.0	80.0	0.0	80.0	35.0
		H_r-2	160.0				31.5
		H_r-3	160.0				10.0
5/01	Plate 01, left upper corner, line 3, 300 mm	H_r-1	85.0	0.0	75.0	75.0	22.0
		H_r-2	85.0				30.0
		H_r-3	160.0				63.0
6/01	Plate 01, right upper corner, line 3, 340 mm	H_r-1	100.0	0.0	230.0	230.0	30.0
		H_r-2	100.0				51.0
		H_r-3	330.0				68.0
7/01	Plate 01, left lower corner, line 4, 300 mm	H_r-1	0.0	0.0	0.0	0.0	34.0
		H_r-2	0.0				32.0
		H_r-3	0.0				11.0
8/01	Plate 01, right lower corner, line 4, 340 mm	H_r-1	244.0	0.0	80.0	80.0	40.0
		H_r-2	244.0				53.0
		H_r-3	164.0				49.0
9/01	Plate 01, forcing in ϕ10, 1 N, $\sim$200 mm	H_r-1	208.0	33.0	32.0	65.0	26.0
		H_r-2	175.0				37.0
		H_r-3	143.0				16.0
10/01	Plate 01, welding in ϕ10, $\sim$300 mm	H_r-1	-261.0	39.0	12.0	27.0	57.0
		H_r-2	-300.0				60.0
		H_r-3	-288.0				52.0

The scanning on the centre line of the plate disclosed two welded joints of the parallelepiped, the vicinities of the forced in pin and two welded joints of the next pin.

The existence of welded joints is characterised by great changes of H_r value and accompanied surges of value $dH/dx = K$ which take the values 54 and 45 for the parallelepiped and 60 or 50 for the welded pin and for the forced in pin $K = 37\,(\mathrm{A/m})/\mathrm{mm}$, see Fig. 5.

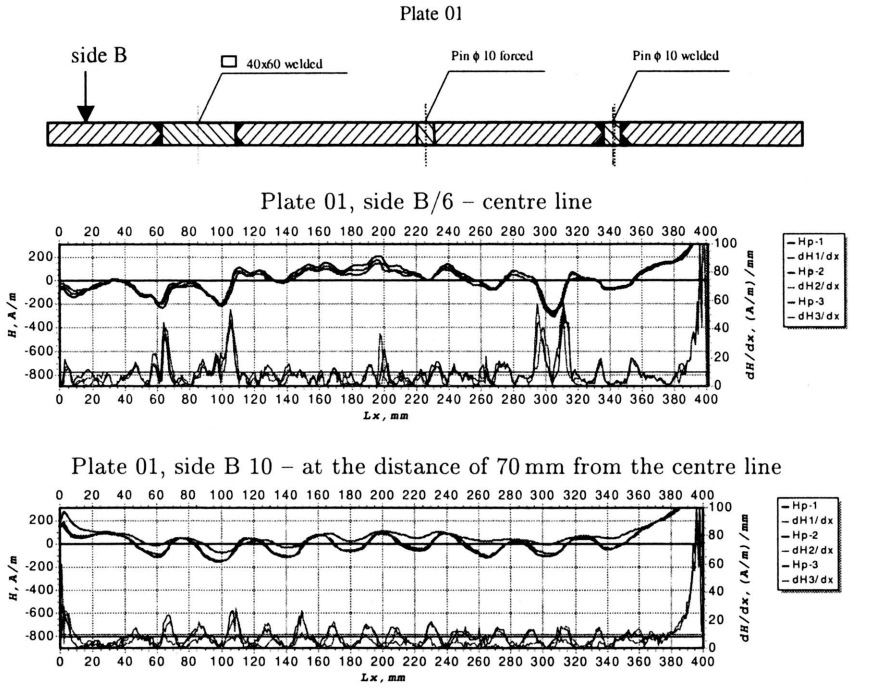

FIGURE 5. Distribution of residual magnetism for the plate 01.

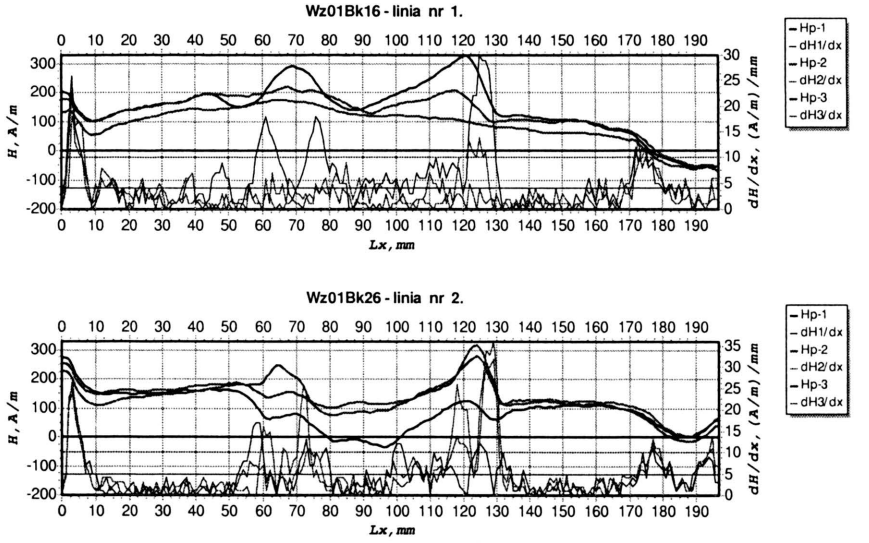

FIGURE 6. Distribution of residual magnetism for the plates 01Bk, 16 and 26 – transverse welds.

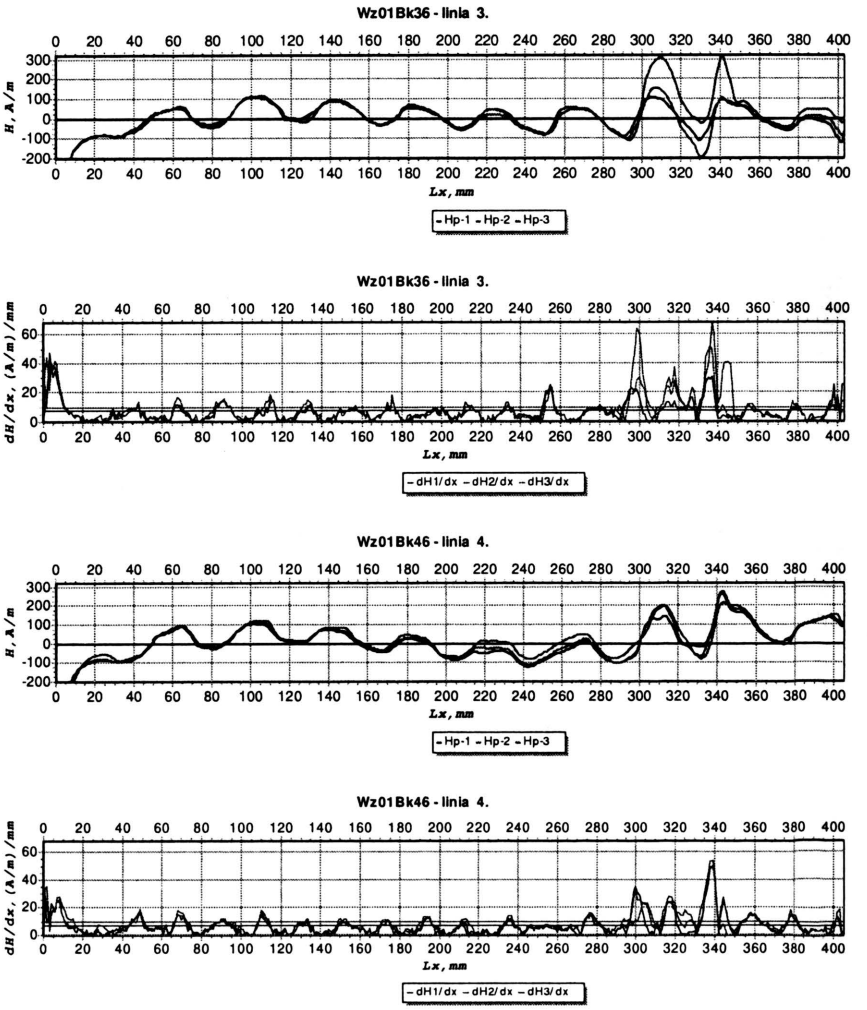

FIGURE 7. Distribution of residual magnetism for the plates 01Bk, 36 and 46 – longitudinal welds.

As results from the X-ray scans and the values of K presented above, its level testifies about the quality of performed joints, e.g. the existence of defects and accompanied stress concentration.

The scanning with multi-channel sensor (in this case 3 channels) gives the idea about an extent and form of defects and associated stress concentration zones. The geometry is reflected by overlaying maximum values of K in particular channels for parallelepiped welded joints and by their shifting against each other in the case of the pin.

It is visible in the X-ray scans that the biggest defects in the parallelepiped welded joints occur at its corners. To corroborate this statement the scans were made along all welded joints and lines 1 and 2 are positioned along the welds which are in transverse position against the plate and line 3 and 4 for the welds which are along it.

As results from included H_r^y values and Table 1 for the values of K the worst joint quality happens at the upper-right corner and the X-ray picture confirms it in Fig. 4.

3.2. Steel plate 02 as above – Figs. 8 and 9 with:

- welded joint $\phi 10$ mm,
- surfacing by welding along the transverse line with 1 mm width cut nick located at the base of triangle notch,
- forced in pin $\phi 5$ mm.

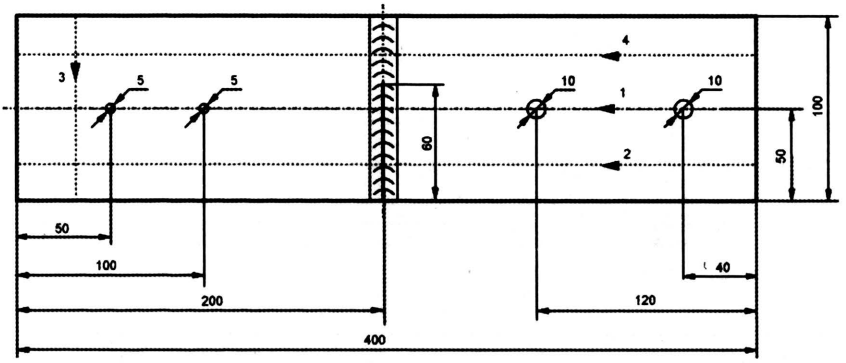

FIGURE 8. Plate 02 with designed defects.

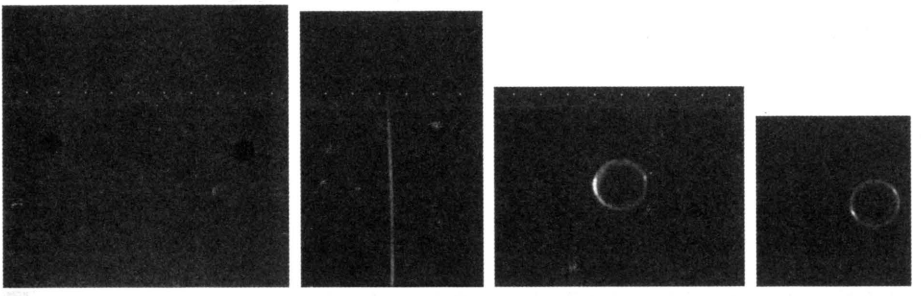

FIGURE 9. X-ray scans of 02 plate with performed defects.

Test results are presented in Figs. 10 and 11 and in Table 2.

TABLE 2.

No.	Type of defect	No. of channel	H	$\lvert H_2 - H_1 \rvert$	$\lvert H_2 - H_3 \rvert$	$\lvert H_1 - H_3 \rvert$	$K_{\max}$
1/01	Plate 02, welded joint $\phi 10$, ~ 120 mm (Figs. 8, 6)	H_r-1	-27.0	14.0	33.0	53.0	11.000
		H_r-2	-7.0				9.000
		H_r-3	26.0				3.100
2/01	Plate 02, surfacing by welding and with a nick ~ 200 mm (Figs. 8, 6)	H_r-1	12.0	3.0	6.0	3.0	9.000
		H_r-2	9.0				6.000
		H_r-3	15.0				8.000
3/01	Plate 02, forcing in $\phi 5$, 2 N, ~ 300 mm, (Figs. 8, 6)	H_r-1	-39.0	35.0	0.0	35.0	13.000
		H_r-2	-4.0				7.000
		H_r-3	-4.0				3.000

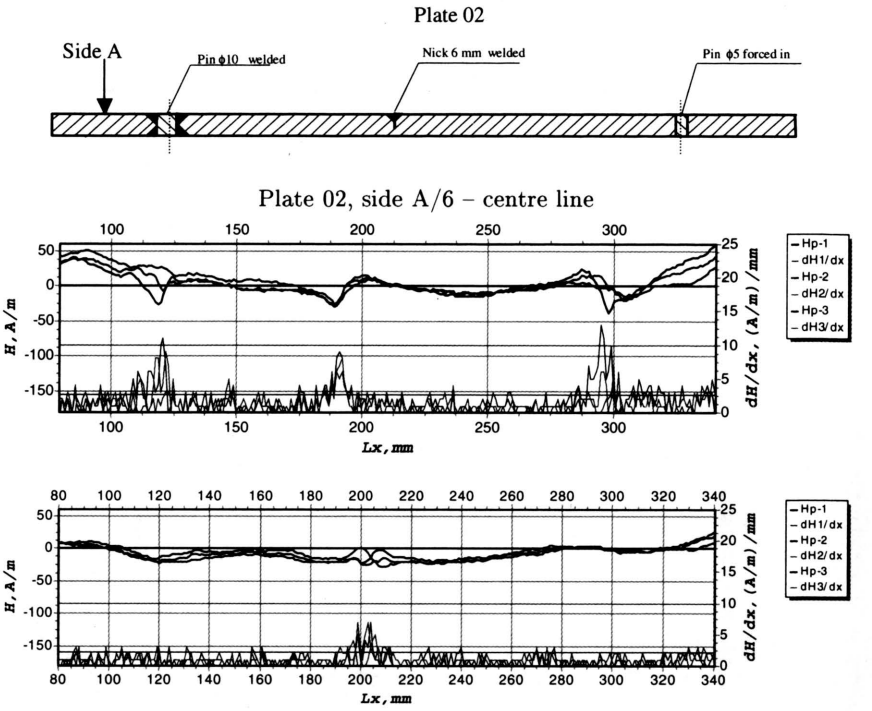

FIGURE 10. Distribution of residual magnetism in plate 02 – three measurement channels.

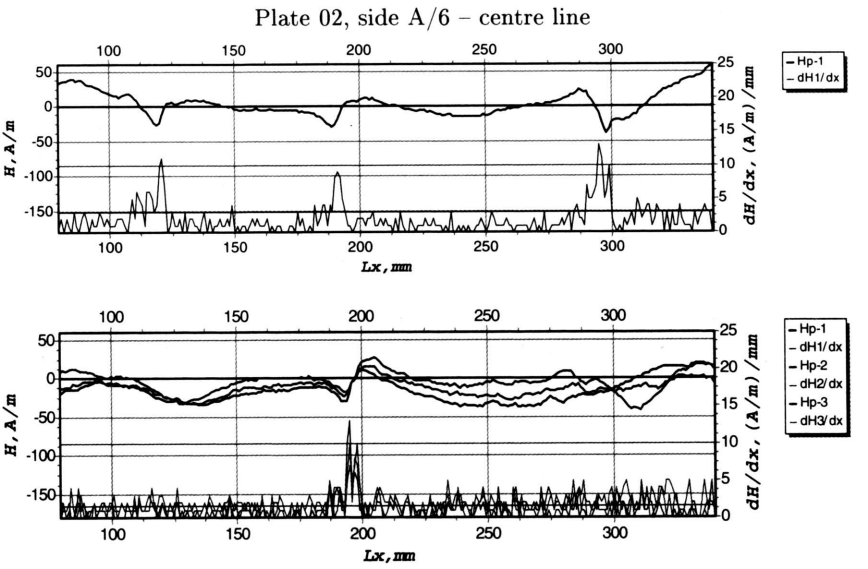

FIGURE 11. Distribution of residual magnetism in plate 02 – one measurement channels.

Scanning along the centre line of the plate (Fig. 6) has disclosed the welded joint of the pin ($K_{\max} = 11$), forced-in joint ($K_{\max} = 13$) and the surfacing by welding with the transverse nick ($K_{\max} = 9$). Maximum values of K are shifted against each other in the case of welded and forced-in joints. In the case of surfacing by welding with the nick they overlay and this witnesses about the geometry of existing defects and stress concentration zones associated with them.

Scanning along the line 2 (Fig. 6) that runs by surfacing by welding with a nick disclosed their presence through the sudden change of H_r^y value and the pick coefficient $K = 13\,(\mathrm{A/m})/\mathrm{mm}$ and they are clearly discerned on the neighbour background.

However, the scanning along the line 3 (Fig. 6) only through the surfacing by welding without the nick disclosed this joint by smaller changes in H_r^y and the values of the coefficient K ($\sim 7\,(\mathrm{A/m})/\mathrm{mm}$) values.

3.3. Steel plate 04 – Fig. 12, as above

6 pins with the diameter 12 mm is forced in this plate.

The results of tests are presented in Fig. 13 and Table 3.

Scanning along the line 1 (see Fig. 12) disclosed forced-in joints for successive pins a, b and c. The force of their forcing-in was 3 N, 1 N and 2 N respectively.

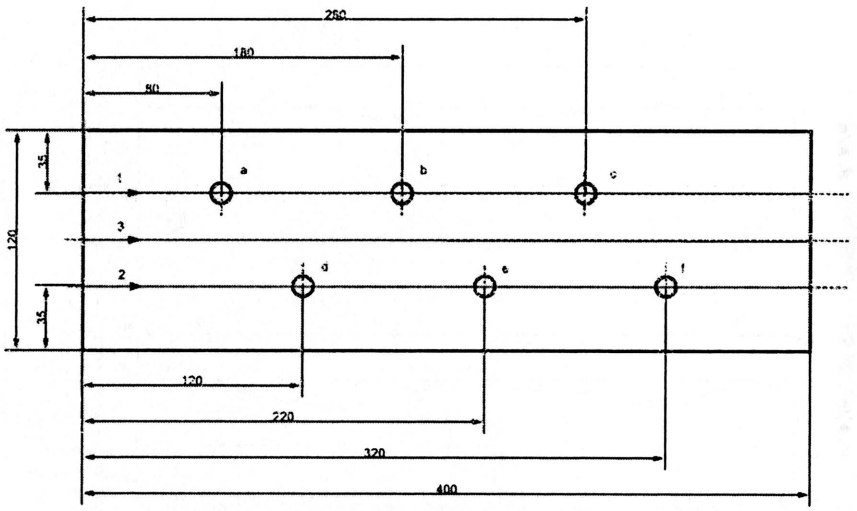

FIGURE 12. Plate 04 with introduced defects in the form of forced-in pins.

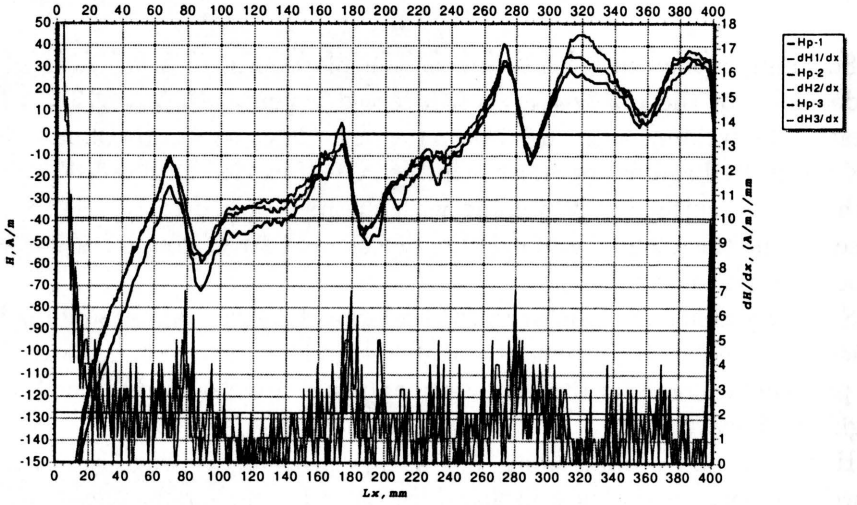

FIGURE 13. Distribution of residual magnetism for the plate 04.

The above joints are reflected by sudden changes of H_r^y and the coefficient K corresponding to them are also clearly visible although their values are relatively small ($\sim 7\,(\mathrm{A/m})/\mathrm{mm}$) and almost equal for all joints.

The forcing-in with the force of 3 N is characterised by the largest difference $|H_1 - H_3|$ between channels and is 16 A/m where for the remaining joints we get 4.0 and 3.0 respectively.

TABLE 3.

No.	Type of defect	No. of channel	H	$\lvert H_2 - H_1 \rvert$	$\lvert H_2 - H_3 \rvert$	$\lvert H_1 - H_3 \rvert$	$K_{\max}$
1/04	Plate 04, forcing in ϕ12, No. 1, 60-100 mm, 6 mm	H_r-1	-72.0	13.0	3.0	16.0	7.000
		H_r-2	-59.0				5.000
		H_r-3	-56.0				4.000
2/04	Plate 04, forcing in ϕ12, No. 2, 160-200 mm, 6 mm	H_r-1	-51.0	6.0	2.0	4.0	7.000
		H_r-2	-45.0				6.000
		H_r-3	-47.0				6.000
3/04	Plate 04, forcing in ϕ12, No. 3, 260-300 mm, 6 mm	H_r-1	-14.0	4.0	1.0	3.0	7.000
		H_r-2	-10.0				5.000
		H_r-3	-11.0				5.000

4. The burning chamber shown Fig. 14

After carrying out the motor trial on the motor test bench what means that the burning chamber was exposed to high pressures and temperatures the zones of H_r value rapid changes appeared in all measurement channels

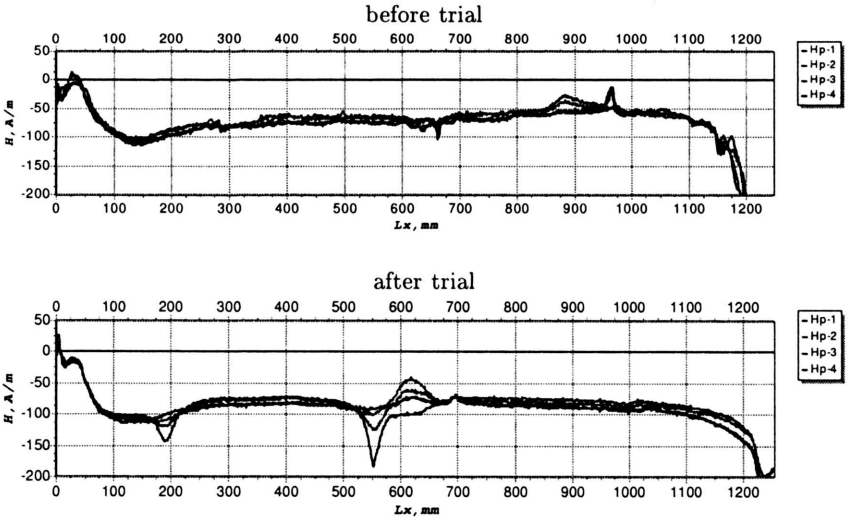

FIGURE 14. The burning chamber before and after test – line "d".

like $\sim$ 200 mm and 550-650 mm. The circumference joints are in disclosed places which integrate particular units of burning chamber.

The values of dH/dx were small in this case, below 10 (A/m)/mm, and they were equally distributed and could not be used as a criterion for distinguishing the above joints.

5. High pressure spherical air containers shown in Fig. 15

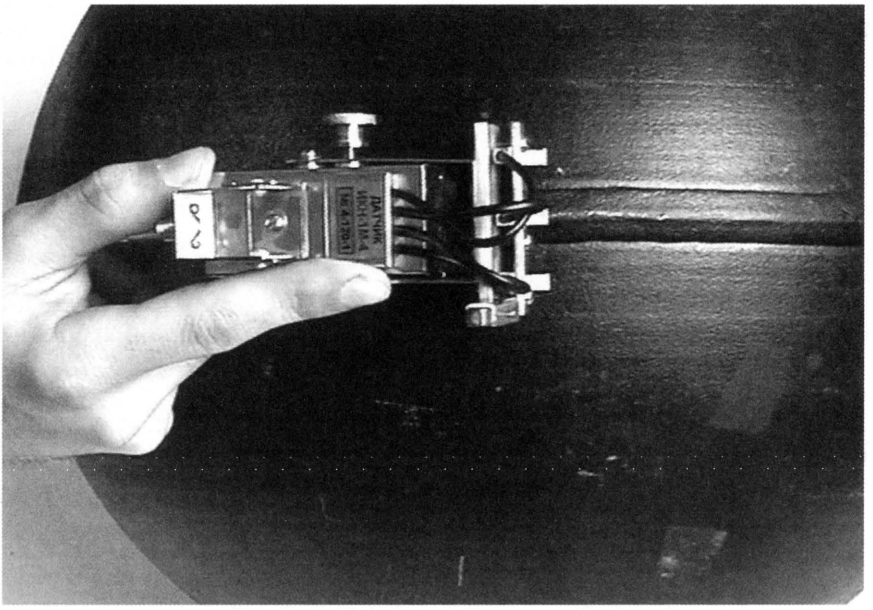

FIGURE 15. Welded container tested by 1 type sensor.

There were 30 containers which have undergone tests and a few of them are presented in Fig. 16. Moreover, the correctly welded container No. 5496 is represented in Fig. 17 and the incorrectly welded ones with Nos. 2171 and 6081 in Fig. 18 and in Table 4.

Container No. 6521 has undergone the hydraulic trial up to 55 MPa pressure. The distribution of residual magnetism for this container before, under and after the trial is presented in Fig. 19. The defect located in the zone of 700-750 mm remains and the stress concentration zone appears in the region of 50-100 mm what is visible after more detailed study of values of H_r.

There are measurement results of H_r^y along the circumference weld for a few containers presented in Fig. 17 which were selected from a few dozen tested ones. Figure 18 presents two of them with weld defects. They were indicated by the rapid changes of H_r^y in the second channel for the boundary

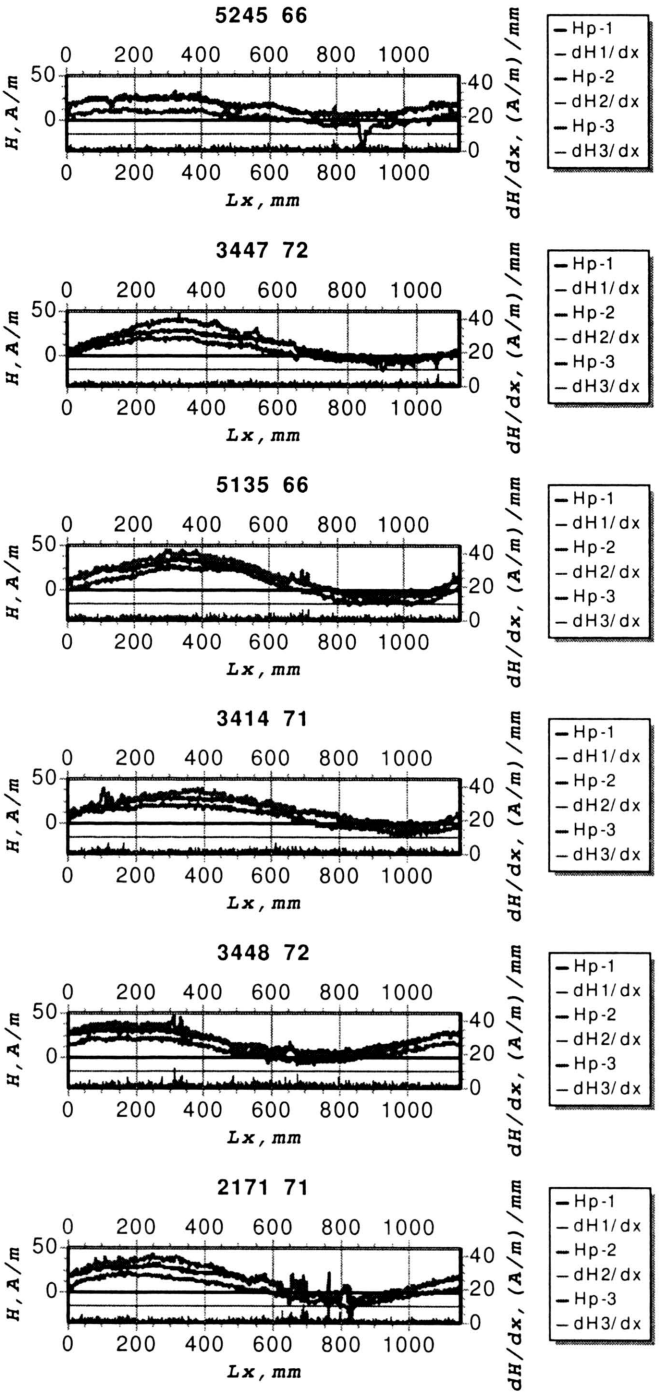

FIGURE 16. Steel ball containers – circumference weld.

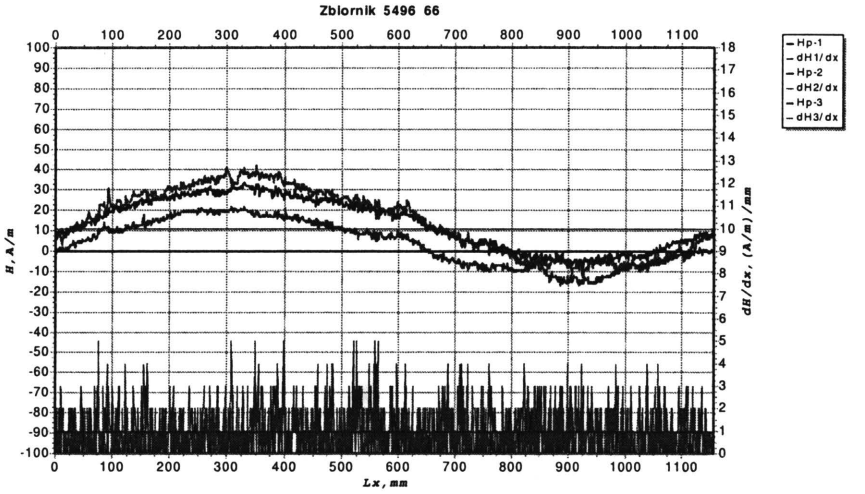

FIGURE 17. Container with a correct weld.

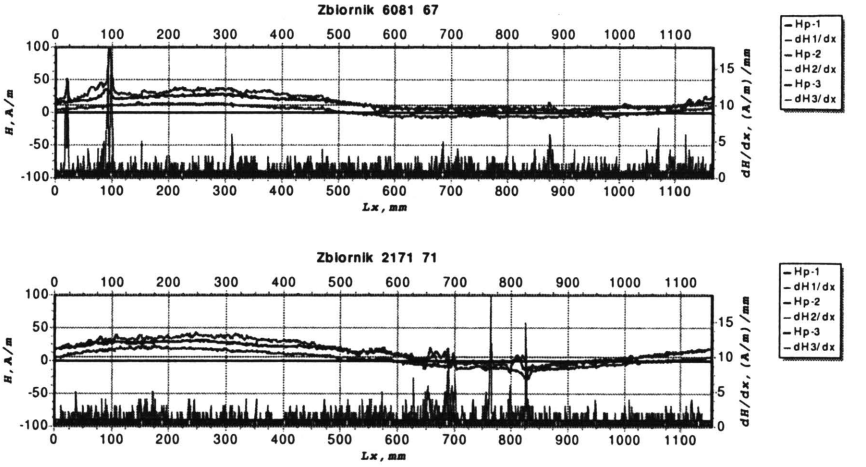

FIGURE 18. Containers with incorrect welds.

TABLE 4.

No.	Type of defect	No. of channel	H	$\lvert H_2 - H_1 \rvert$	$\lvert H_2 - H_3 \rvert$	$\lvert H_1 - H_3 \rvert$	$K_{\max}$
1.	Cylinder No. 2171, ~825 mm, with defect	H_r-1	-13.0	14.0	0.0	14.0	3.0
		H_r-2	-27.0				15.0
		H_r-3	-27.0				4.0
2.	Cylinder No. 2171, ~760 mm, with defect	H_r-1	-5.0	27.0	36.0	9.0	5.000
		H_r-2	22.0				19.000
		H_r-3	-14.0				7.000
3.	Cylinder No. 6081, with defect ~20 mm	H_r-1	16.0	35.0	46.0	11.0	3.000
		H_r-2	51.0				12.000
		H_r-3	5.0				2.000
4.	Cylinder No. 6081, 100 mm	H_r-1	35.0	65.0	87.5	22.5	5.000
		H_r-2	100.0				16.000
		H_r-3	12.5				3.000
5.	Cylinder No. 6521, before trial 0.0 MPa, ~710 mm	H_r-1	-19.0	6.0	27.5	33.5	6.000
		H_r-2	-13.0				10.000
		H_r-3	14.5				4.000
6.	Cylinder No. 6521, pressure: 55 MPa, ~710 mm	H_r-1	-27.0	38.5	6.5	45.0	9.000
		H_r-2	11.5				6.000
		H_r-3	18.0				4.000
7.	Cylinder No. 6521, after trial 0.0 MPa, ~710 mm	H_r-1	-27.0	39.8	3.9	43.7	8.000
		H_r-2	12.8				6.000
		H_r-3	16.7				5.000

between the weld and welded material and also for the first and third channels what suggests that those defects include also the heat influence zone. Rapid changes of the coefficient K were observed. For instance, $K_{\max} = 16.0$ for the container No. 6081 and $K_{\max} = 19$ for No. 2171.

The pressure trial carried out for container No. 6521 has confirmed that its residual magnetism is due, first of all, to maximal stresses at pressure trial performed by the manufacturer under 52.5 MPa. Only above this value (55 MPa) some small changes of H_r^y distribution become visible along the weld.

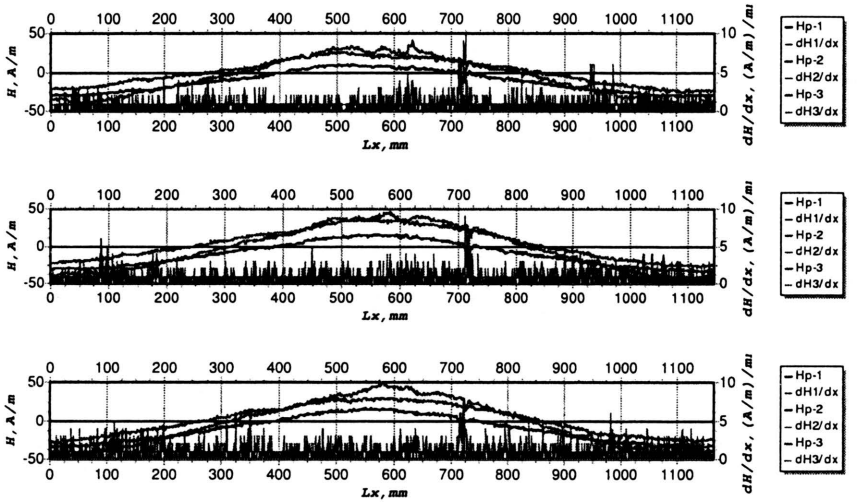

FIGURE 19. Measurement results taken before, under and after the pressure trial of the container No. 6521.

6. Conclusions

It is possible to draw the following conclusions considering the presented results:

- the defects of welded joints are characterised by sudden changes of H_r^y, including the change of sign. High values of K_{in} are linked with it reaching at some cases the level of 50 (A/m)/mm,
- in the case of surfacing by welding the conclusion is similar and the presence of defects was confirmed by X-ray scans,
- forcing-in introducing the stresses is characterised by quick change of H_r^y with associated high values for the coefficient K_{in}.

Relative to the burning chamber we conclude that:

- the existence of stresses expressed by quick changes of H_r^y in all channels at the distances 250 and 580 and 680 from the scanning start point. The values of the coefficient K_{in} are small and less than 10 (A/m)/mm. In disclosed places the welding seam of the ring for rear and front part of burning chamber connection was discovered.

Relative to the air cylinders we conclude that:

- quick changes of H_r^y for the weld and welded material boundary and heat influence zone, cylinder No. 2171, dH/dx about 12 (A/m)/mm, cylinder No. 6081.

Relative to the performed forcing-in of pins we found that:

- they are characterised by the quick change of H_r^y associated with high value of the coefficient K_{in}. X-ray scans indicate a numerous defects of such joints.

The ultrasonic tests showed that:

- material structural changes connected with the joint repair and point defects as probable corrosion sources in the cylinder No. 2171,
- extensive concentration of point defects as probable corrosion sources in the cylinder No. 6081,
- point defects situated in the weld seam remaining during the trial and visible after the trial and point defects in the boundary between the seam and welded material.

Moreover, ultrasonic tests disclosed numerous defects in welded joints and most of them are due to the lack of melting. In what concerns the forcing-in joints there were defects connected with imperfect machining. The results of those tests coincide with the results obtained by the metal magnetic memory method.

References

(All publications in Polish or Russian)

1. Z. BRZOSKA, *Wytrzymałość materiałów*, PWN, Warszawa 1972.
2. Z. KLĘBOWSKI, *Wytrzymałość przemysłowych naczyń cisnieniowych*, PWT, Warszawa 1960.
3. W. NOWACKI, *Teoria sprężystości*, PWN, Warszawa 1970.
4. A. MORRISH, *Fizyczne podstawy magnetyzmu*, PWN, Warszawa 1970.
5. A.A. DOUBOV, *Mietod magnitnoj pamiati metalla i pribory kontrolia* (in Russian), Energodiagnostika, Moscow 2001.
6. A.A. DUBOW, *Diagnostyka przewodów rurowych, oprzyrządowania i konstrukcji z wykorzystaniem magnetycznej pamięci metalu*, Metal Science, Warszawa 1999.
7. *Wskaźniki metodyczne do technicznego diagnozowania połączeń spawanych, przewodów rurowych i walczaków z wykorzystaniem metody magnetycznej pamięci metalu*, Metal Science, Warszawa 1999.
8. E.M. PURCELL, *Elektryczność i magnetyzm*, PWN, Warszawa 1971.
9. K. WESOŁOWSKI, *Metaloznawstwo*, WAT, Warszawa-Bemowo 1953.